Luminosity Dependence

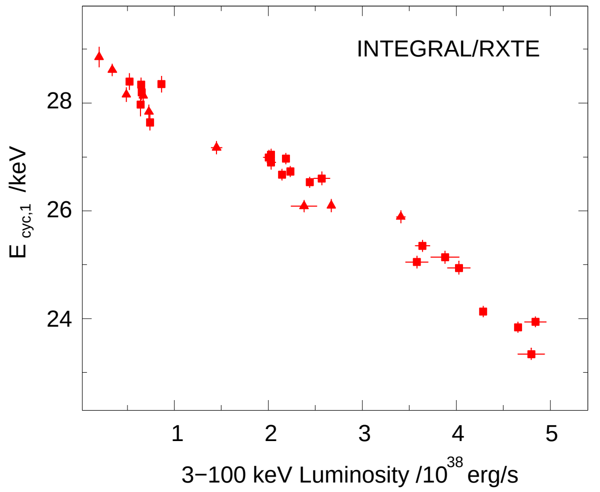

V0332+53: Cyclotron line energy depends on luminosity

$\Longrightarrow$ change of height of accretion column with $\dot{M}$

(Tsygankov et al., 2006)

Luminosity Dependence

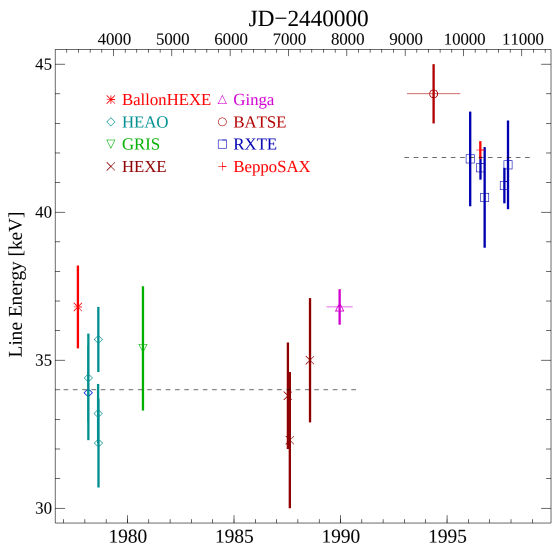

The cyclotron line in Her X-1 shows significant secular variability!

Gruber et al. (2002)

Luminosity Dependence

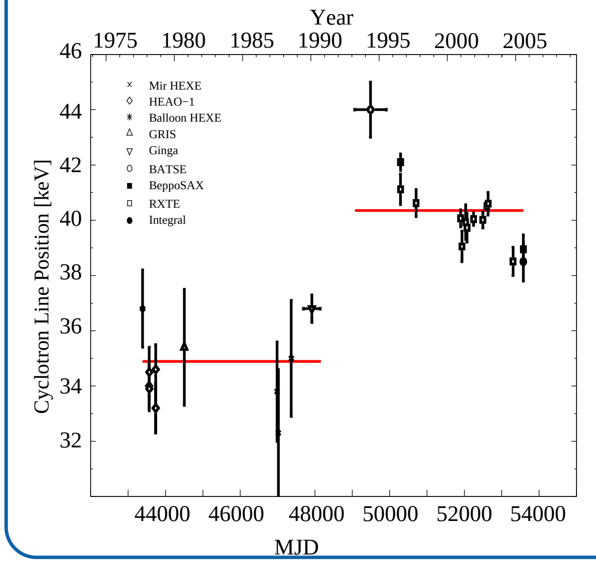

The cyclotron line in Her X-1 shows significant secular variability!

Staubert et al. (2007)

Luminosity Dependence

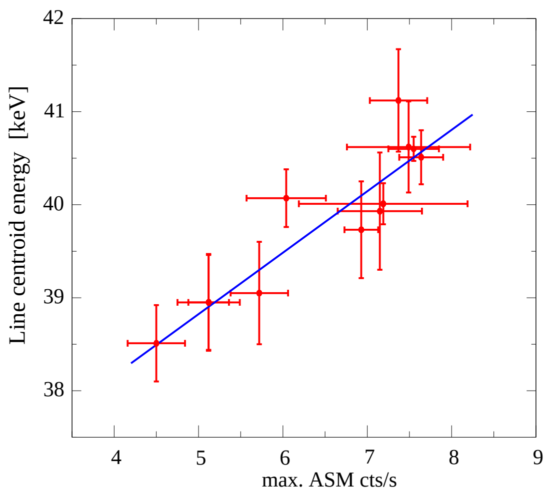

. . . but the dependence of E_{cyc} on L is different than in high luminosity sources

Her X-1: sub-Eddington source

$\Longrightarrow$ need to take structure of accretion mound into account

$\Longrightarrow$ dynamic pressure of infalling protons results in *decrease* of height of accretion mound with increasing L!

Staubert et al. (2007)

Araya, R. A., & Harding, A. K., 1999, ApJ, 517, 334

Arons, J., Klein, R. I., & Lea, S. M., 1987, ApJ, 312, 666

Basko, M. M., & Sunyaev, R. A., 1976, MNRAS, 175, 395

Becker, P. A., 1998, ApJ, 498, 790

Becker, P. A., & Wolff, M. T., 2005a, ApJ, 621, L45

Becker, P. A., & Wolff, M. T., 2005b, ApJ, 630, 465

Becker, P. A., & Wolff, M. T., 2007, ApJ, 654, 435

Bildsten, L., et al., 1997, ApJS, 113, 367

Braun, A., & Yahel, R. Z., 1984, A&A, 278, 349

Caballero, I., et al., 2007, A&A, 465, L21

Canuto, V., 1970, ApJ, 160, L153

Canuto, V., Lodenquai, J., & Ruderman, M., 1971, Phys. Rev. D, 3, 2303

Charles, P. A., & Seward, F. D., 1995, Exploring the X-Ray Universe, (Cambridge: Cambridge Univ. Press)

Davidson, K., & Ostriker, J. P., 1973, ApJ, 179, 585

Fritz, S., Kreykenbohm, I., Wilms, J., Staubert, R., Bayazit, F., Rodriguez, J., & Santangelo, A., 2006, A&A, 458, 885

Ghosh, P., & Lamb, F. K., 1979, ApJ, 232, 239

Gnedin, Y. N., & Sunyaev, R. A., 1973, A&A, 25, 233

Gonthier, P. L., Harding, A. K., Baring, M. G., Costello, R. M., & Mercer, C. L., 2000, ApJ, 540, 907

Harding, A. K., 1994, in The Evolution of X-Ray Binaries, ed. S. S. Holt, C. S. Day, (Washington: AIP), 429

Heindl, W. A., Rothschild, R. E., Coburn, W., Staubert, R., Wilms, J., Kreykenbohm, I., & Kretschmar, P., 2004, in AIP Conf. Proc. 714: X-ray Timing 2003: Rossi and Beyond, ed. P. Kaaret, F. K. Lamb, J. H. Swank, 323

Inoue, H., 1975, PASJ, 27, 311

Kreykenbohm, I., Kretschmar, P., Wilms, J., Staubert, R., Kendziorra, E., Gruber, D., & Rothschild, R., 1999, A&A, 341, 141

Langer, S. H., & Rappaport, S., 1982, ApJ, 257, 733

Mészáros, P., 1984, Space Sci. Rev., 38, 325

Mészáros, P., 1992, High-energy radiation from magnetized neutron stars, (Chicago: Chicago Univ. Press)

Mészáros, P., & Nagel, W., 1985a, ApJ, 298, 147

Mészáros, P., & Nagel, W., 1985b, ApJ, 299, 138

Mowlavi, N., et al., 2006, A&A, 451, 817

Nagel, W., 1981a, ApJ, 251, 278

Nagel, W., 1981b, ApJ, 251, 288

Ostriker, J. P., & Davidson, K., 1973, in X- and Gamma-Ray Astronomy, ed. H. Bradt, R. Giacconi, 143

Pottschmidt, K., et al., 2005, ApJ, 634, L97

Pringle, J. E., & Rees, M. J., 1972, A&A, 21, 1

Rappaport, S., & Joss, P. C., 1977, Nature, 266, 683

Schönherr, G., Wilms, J., Kretschmar, P., Kreykenbohm, I., Santangelo, A., Rothschild, R. E., Staubert, R., & Coburn, W., 2007, A&A, submitted

Trümper, J., Pietsch, W., Reppin, C., Voges, W., Staubert, R., & Kendziorra, E., 1978, ApJ, 219, L105

Tsygankov, S. S., Lutovinov, A. A., Churazov, E. M., & Sunyaev, R. A., 2006, MNRAS, 371, 19

Ventura, J., 1979, Phys. Rev. D, 19, 1684

Low-Mass X-ray Binaries

Introduction

We now turn to older neutron stars in low mass X-ray binaries (LMXBs).

These systems have lower B-fields
$\Longrightarrow$ no pulsations observed

What we will talk about:

- Spectral Shape/ Classification
  Atoll-sources, Z-sources, Dippers
- X-ray Bursts
- Rapid Time Variability
- Accretion Disk Corona Sources

Table 1 Bright low-mass X-ray binaries[a]

Source name(s)	l^{II}, b^{II} (°)	I_x[b] Mean (μJy)	Min. (μJy)	Max. (μJy)	P_{orb}[c] (hr)	Type[d]	Phenomenology[e]
Sco X-1 (1617−155)	359+24	12,400	9300	16,300	19.2	Z	QPO
GX 5−1 (1758−250)	5−1	1200	1070	1410	—	Z	QPO
GX 349+2 (1702−363)[f]	349+3	780	620	980	—	Z	QPO
GX 17+2 (1813−140)	16+1	680	600	780	19.8?[g]	Z	QPO, (bu)
GX 9+1 (1758−205)	9+1	650	550	720	—	A	—
GX 340+0 (1642−455)	340−0	490	400	620	—	Z	QPO
GX 3+1 (1744−265)	2+1	430	230	550	—	A	QPO, (Bu)
Cyg X-2 (2142+380)	87−11	430	290	730	235	Z	QPO, (bu), Mo
GX 13+1 (1811−171)	14+0	340	240	430	—	A	—
GX 9+9 (1728−169)	8+9	290	230	340	4.2	A	Mo
4U 1820−30 (NGC 6624)	3−8	260	94	360	0.2	A	QPO, (Bu), Mo
4U 1705−44	343−2	260	39	440	—	A	Bu
4U 1636−53	333−5	220	100	320	3.8	A	Bu
Ser X-1 (1837+049)	36+5	200	150	290	—	—	Bu
GCX-1 (1742−294)	0−0	170	130	270	—	—	Bu?
4U 1728−33	354−0	170	140	190	—	A	Bu
GX 339−4 (1659−487)	339−4	160	36	250	14.8?	—	QPO, BH?[h]
4U 1735−44	346−7	160	110	210	4.6	A	Bu

[a] All variable objects in 3A Catalogue (69, 153) with an average flux ≥100 μJy not identified with an early-type star (excluding Cyg X-3).
[b] Converted from *Ariel V* ASM counts into μJy (2–11 keV) according to 1 ASM c/s = 2.6 μJy (9).
[c] See (84).
[d] Z or A(toll) source; see text. After (36).
[e] QPO: all reported quasi-periodic oscillations are indicated here (see Section 3 for an evaluation of QPO reports in atoll sources); Bu: regular X-ray bursts; (Bu): has shown an episode of regular X-ray bursts; (bu): occasional X-ray bursts reported; BH?: black hole candidate, Mo: shows periodic X-ray modulation (9, 55, 64).
[f] "Sco X-2."
[g] Reference: (37).
[h] References: (77, 157).

(van der Klis, 1989, Tab. 1)

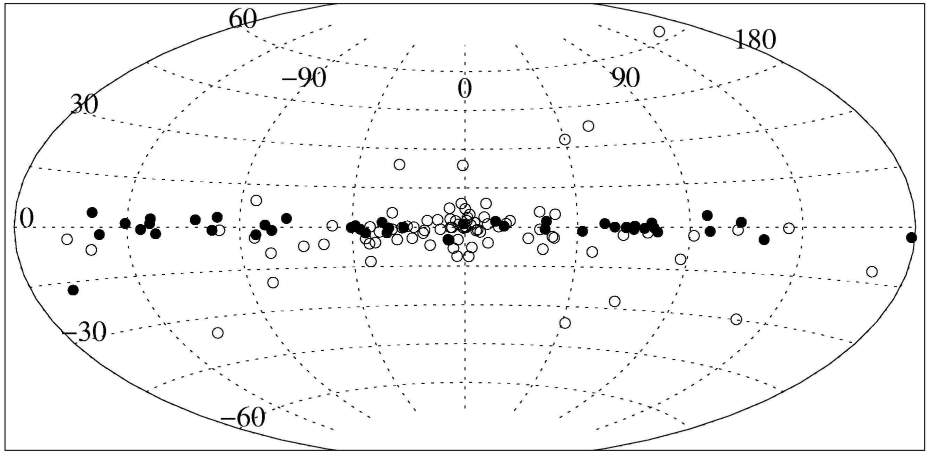

(Grimm, Gilfanov & Sunyaev, 2003)

Distribution of HMXB (filled circles) and LMXB (open circles) in the Galaxy

Classification

Hasinger & van der Klis (1989): "Two patterns of correlated X-ray timing and spectral behaviour in low-mass X-ray binaries"

Source classification through their behavior in the color-color-diagram or in the Hardness-Intensity-Diagram:

Here, we define an X-ray color (or "hardness ratio"):

$$\text{color} = \frac{\text{CR}_{\text{upper energy band}}}{\text{CR}_{\text{lower energy band}}} \quad (6.1)$$

where CR_i is the measured count rate in a given energy band.

Typical bands used depend on the satellite, typical width is a few keV!

Z-sources, I

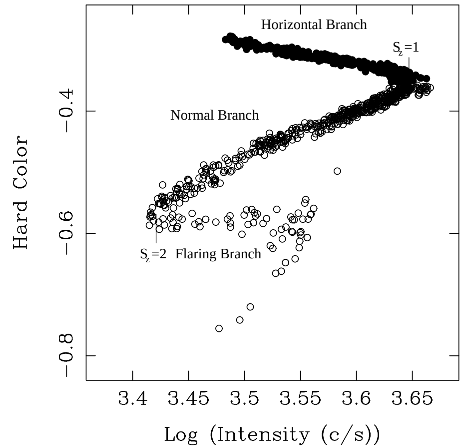

(GX 340+0; Jonker et al., 2000)

Z-sources: higher luminosity LMXBs (L_X close to L_{Edd}).

Color-intensity-diagram:

- horizontal branch: characterized by 20–50 Hz "Horizontal Branch Oscillations" (HBOs) and strong variability (including quasi-periodic oscillations, QPOs)
- normal branch: much weaker variability

  pre 1988 people thought this behavior to be the normal one for neutron star LMXB.
- flaring branch: spectrum mostly thermal

  Named after flares in Sco X-1

Intensity described with S_Z-parameter along the Z.

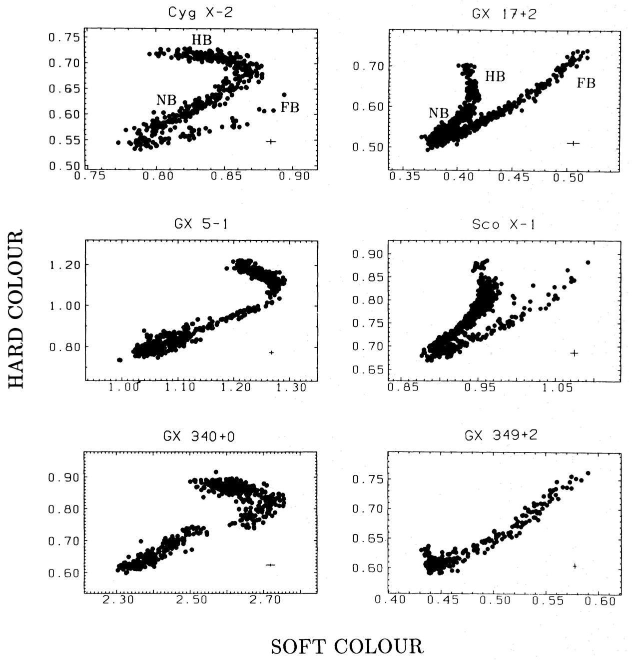

Depending on the source and choice of color bands, the Z is can be rather severely distorted.

(Hasinger & van der Klis, 1989, Fig. 1a)

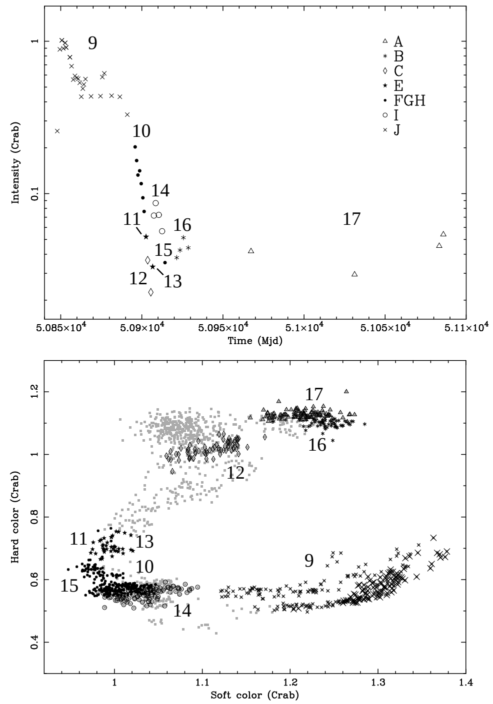

The source location in the color-color diagram varies on timescales of days to weeks

generally slower in island, faster in banana

(van Straaten, van der Klis & Méndez, 2003, Fig. 2)

Atoll sources

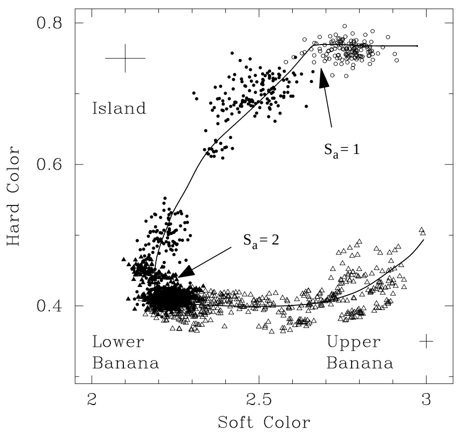

(4U1608−52; Méndez et al., 1999)

Atoll sources: generally lower luminosity than Z-sources; color-color-diagram looks like a pacific island

Intensity increases with parameter S_a:

- banana state: higher luminosity state, variability dominated by low frequency noise
- island state: lower luminosity state, variability dominated by high frequency noise

S_a is defined "by eye", see diagram

Typical luminosities 0.01–0.2 L_{Edd}, although four sources might be brighter than that (van der Klis, 2000)

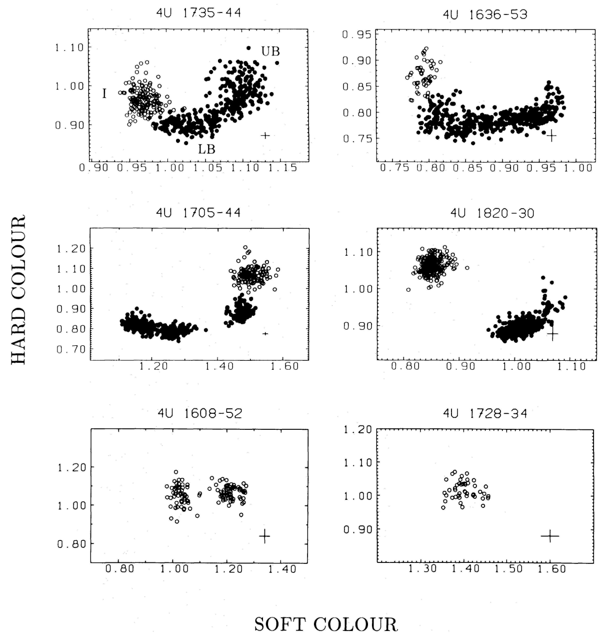

Not all sources are present in the banana and island states, depends on individual source luminosity variations.

(Hasinger & van der Klis, 1989, Fig. 3a)

Spectral shape

(White, Stella & Parmar, 1988): The spectral shape is well described by a power law with exponential cutoff,

$$N_{\mathrm{ph}}(E) \propto E^{-\Gamma} \exp\left(-\frac{E}{E_{\mathrm{fold}}}\right) \quad (6.2)$$

where

- N_{ph}: photon flux (ph cm^{-2} s^{-1} keV^{-1}),
- $\Gamma \sim$ 0–2: photon index,
- $E_{\mathrm{fold}} \sim$ 1–20 keV: folding energy (also often called cutoff energy)

Such a spectral shape probably due to Comptonization

High luminosity sources (=Z-sources) show additional black body component with $kT_{\mathrm{BB}} \sim$ 1–2 keV, contributing 10–70% of the total flux (higher L_{X} implies more BB-flux).

Often, an additional Fe Kα line at 6.4 keV is required.

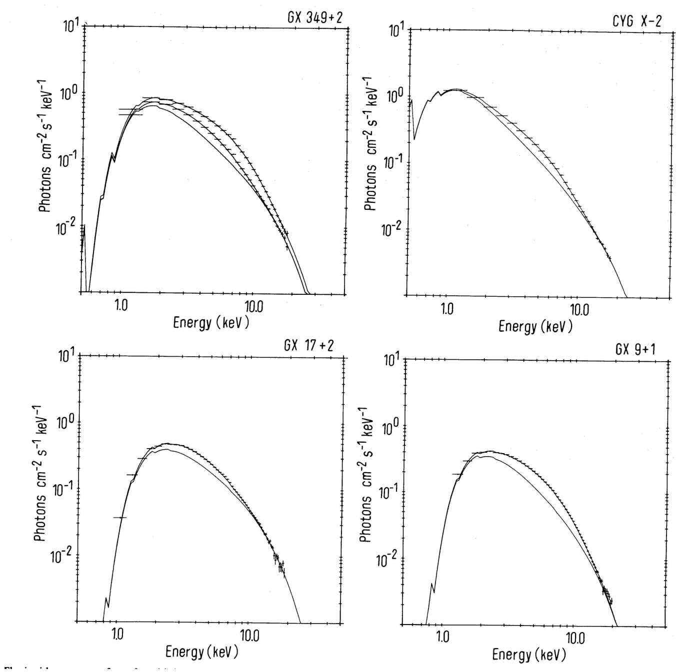

Example spectra of LMXB (White, Stella & Parmar, 1988, lower line is Comptonization only)

Spectral shape

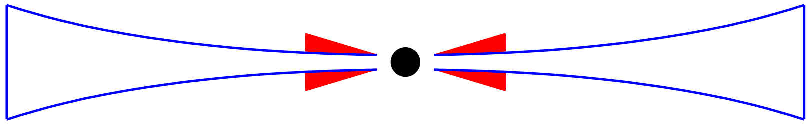

(after Church, 2004)

The interpretation of spectral shape is heavily debated.

Western model (White, Stella & Parmar, 1988) and Birmingham model (Church & Balucinska-Church, 1995):

- black body is from neutron star,
- Comptonization happens in inner edge of the accretion disk (e.g., in hot accretion disk wind).

Spectral shape

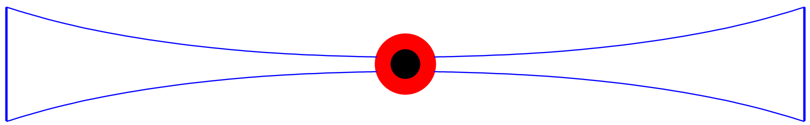

(after Church, 2004)

The interpretation of the spectral shape is heavily debated.

Eastern model (Mitsuda et al., 1989):

- Soft spectrum: thermal radiation from accretion disk

  (assuming $T(r) \propto r^{-3/4}$)

- Hard spectrum is Comptonization in neutron star atmosphere (which provides seed photons as thermal radiation).

X-Ray Bursts

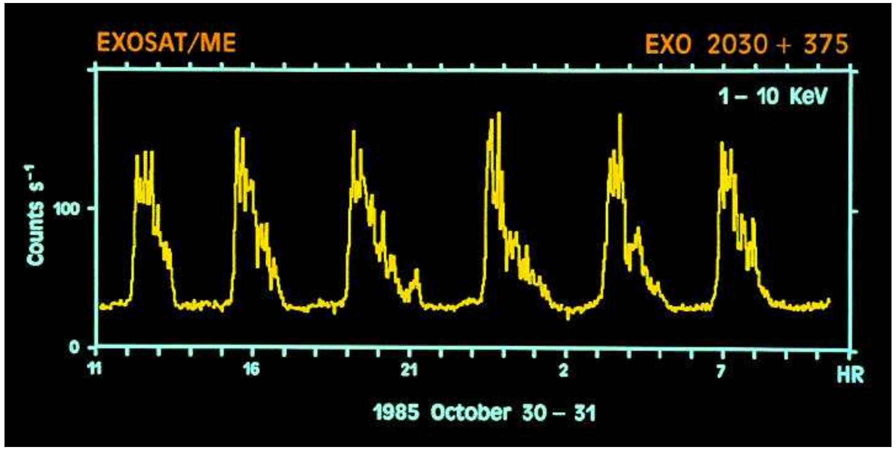

NASA GSFC

X-ray bursts from EXO 2030+375 as seen with EXOSAT.

X-Ray Bursts

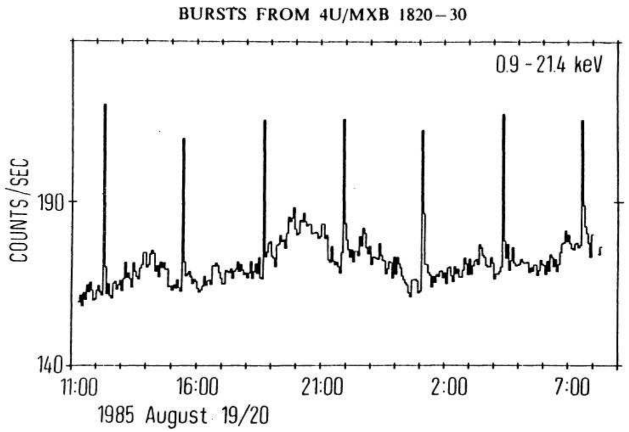

(Lewin, van Paradijs & Taam, 1993, Fig. 3.14b)

Bursts sometimes appear to be regular . . .

Separations down to 10 min are possible.

X-Ray Bursts

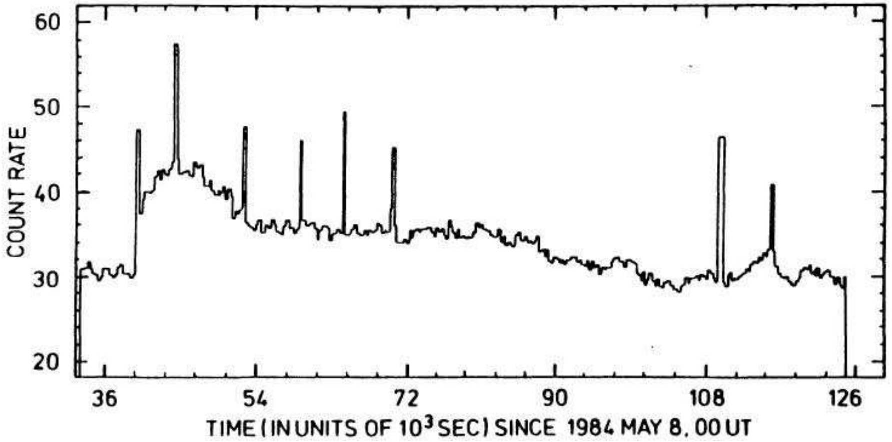

(Lewin, van Paradijs & Taam, 1993, Fig. 3.14b)

. . . and sometimes not.

X-Ray Bursts

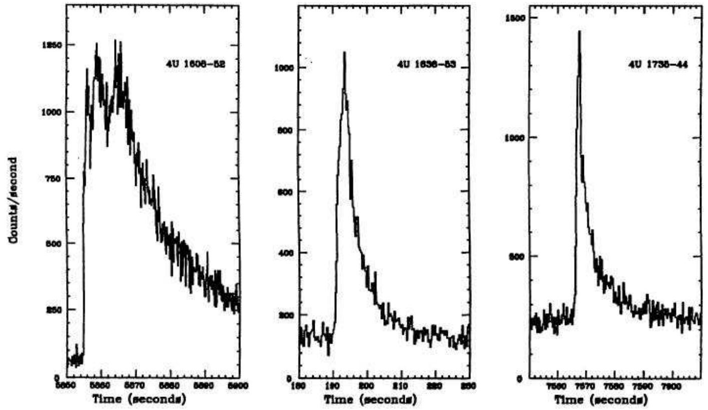

(Lewin, van Paradijs & Taam, 1993, Fig. 3.1)

Bursts come in different shapes, but approximately look like a “FRED”

FRED=Fast Raise and Exponential Decay

X-Ray Bursts

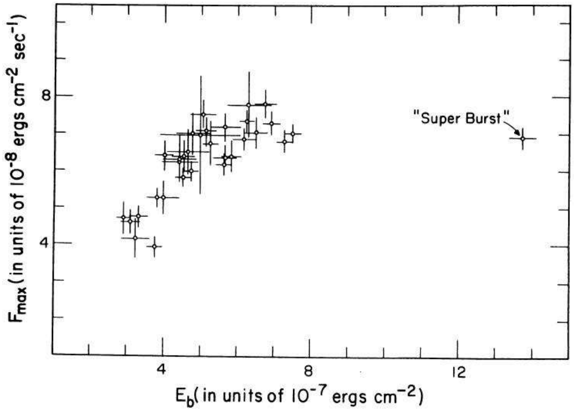

(1728−337; Lewin, van Paradijs & Taam, 1993, Fig. 3.5b)

Peak flux and total fluence of bursts are approxmately linearly correlated
$\Longrightarrow$ more energetic bursts are brighter

X-Ray Bursts

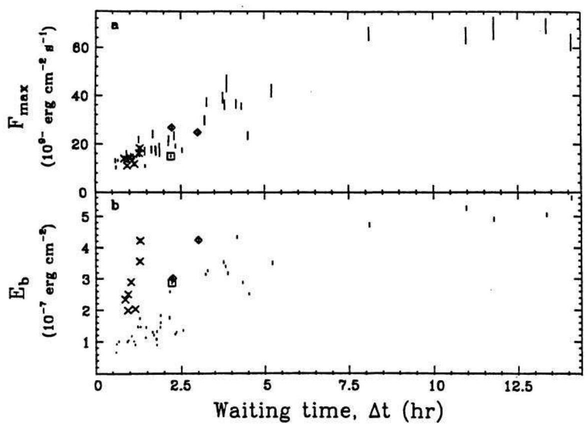

(1636−536; Lewin, van Paradijs & Taam, 1993, Fig. 3.15)

Waiting time and total fluence of bursts are approxmately correlated
$\Longrightarrow$ more energetic bursts come after longer waiting times

X-Ray Bursts

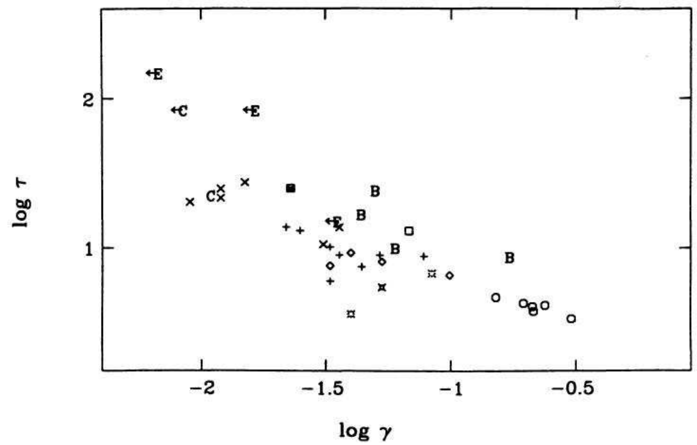

($\gamma = L_X/L_{Edd}$; Lewin, van Paradijs & Taam, 1993, Fig. 3.17)

Waiting times are longer for low luminosity systems, i.e., lower $\dot{M}$.

X-Ray Bursts

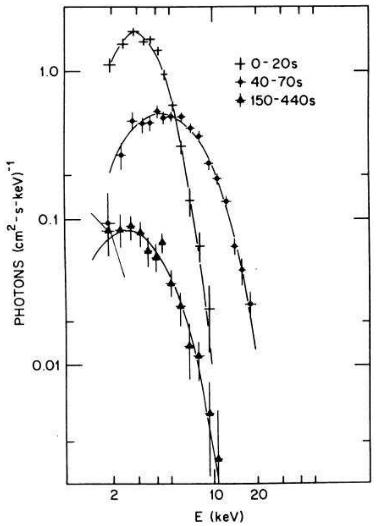

Swank et al. (1977): Spectral shape during the bursts can be well described by a black body spectrum with $kT \sim$ few keV.

$\Longrightarrow$ Optically thick plasma in thermodynamic equilibrium

X-Ray Bursts

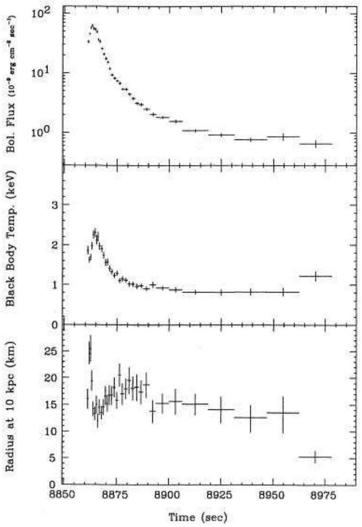

(Lewin, van Paradijs & Taam, 1993, Fig. 3.10)

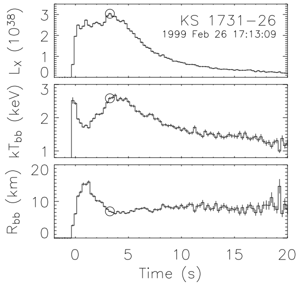

(Galloway et al., 2006, Fig. 1)

Luminosity of a black body: $L_{\text{bb}} = R_{\text{bb}}^2 \sigma T_{\text{bb}}^4$

$\Longrightarrow$ can measure radius of emitter!

$$R = d\sqrt{\frac{4\pi F}{\sigma T^4}}$$

where d estimated distance and F measured flux.

X-Ray Bursts

When looked at in more detail, measuring the temperature during the burst is more complicated:

1. Neutron star is compact, so radiation from surface suffers a gravitational redshift:

$$T_{\text{surface}} = T_{\text{obs}}(1+z) \quad \text{where} \quad 1+z = \left(1 - \frac{2GM}{Rc^2}\right)^{-1/2} \tag{6.3}$$

2. Neutron star atmosphere hardens the surface spectrum through Compton scattering:

$$I_{\text{obs}}(E_{\text{em}}) = B(E_{\text{em}}; T_{\text{eff}})/f^4 \quad \Longleftrightarrow \quad T_{\text{surface}} = fT_{\text{eff}} \tag{6.4}$$

where $B(E,T)$: Black Body spectrum and where

$$f = 1.34 + 0.25((1+X)/1.7)^{2.2}(T_{\text{eff}}/10^7\,\text{K})^4(g/10^{13}\,\text{cm}\,\text{s}^{-2})^{-2.2} \tag{6.5}$$

with $g = (1+z)\cdot GM/R^2$ a correction factor for the surface gravity and $X \sim 0.7$ the atmospheric H-fraction.

Burst Theory, I

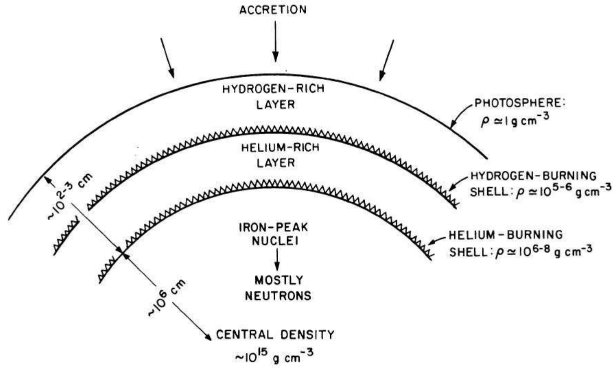

(Joss & Rappaport, 1984, Fig. 13)

Explanation: Bursts are thermonuclear explosions on neutron star surface.

Accretion of hydrogen onto surface $\Longrightarrow$ H fuses into He (mainly electron captures), nuclear statistical equilibrium below that $\Longrightarrow$ He shell, and then higher Z.

Burst Theory, II

Since $T > 10^7$ K: H-burning occurs via the CNO-cycle.

CNO cycle is saturated at $T \gtrsim 8\times 10^7$ K:

timescale for proton capture $<$ β-decays of standard CNO-cycle

$t_{1/2} \sim 100$–1000 s for ^{13}N, ^{14}O, ^{15}O)

$\Longrightarrow$ "hot CNO cycle":

$$^{12}\text{C}(p,\gamma)^{13}\text{N}(p,\gamma)^{14}\text{O}(\beta^+)^{14}\text{N}(p,\gamma)^{15}\text{O}(\beta^+)^{15}\text{N}(p,\alpha)^{12}\text{C}$$

This process is instable for

$$\dot{m} < 900\,\text{g}\,\text{cm}^{-2}\,\text{s}^{-1}(Z_{\text{CNO}}/0.01)^{1/2} \tag{6.6}$$

where Z: mass fraction and where $\dot{m} = \dot{M}/(4\pi R^2)$.

$\Longrightarrow$ Type I burst

Burst Theory, III

For higher $\dot{m}$: H-burning is stable. But: ρ is high, so He burning is also possible (mainly 3α process):

- For $\dot{m} < 2000\,\mathrm{g\,cm^{-2}\,s^{-1}}(Z_{\mathrm{CNO}}/0.01)^{13/18}$:
  H burns faster than He, $\Longrightarrow$ pure He X-ray bursts
- Above this $\dot{m}$: simultaneous H/He-burning.
  Because of the strong temperature dependence of the 3α process:
  - For $T < 5 \times 10^8\,\mathrm{K}$: He ignites explosively in thin shell $\Longrightarrow$ X-ray burst
    conditions typically ok for explosive energy release, once 10^{21} g material have been accumulated; for $\dot{M} \sim 10^{17}\,\mathrm{g\,s^{-1}}$ this corresponds to burst recurrence timescales of 10000 s, as observed; energy release $\sim 10^{39}\,\mathrm{erg\,s^{-1}}$
  - For $T > 5 \times 10^8\,\mathrm{K}$: H and He burns stable
    $\Longrightarrow$ no bursts in higher $\dot{M}$ sources!

see Strohmayer & Bildsten (2006) for recent review and references to current ideas. Early theory (more understandable): Hansen & van Horn (1975), Lamb & Lamb (1978), Taam & Picklum (1979)

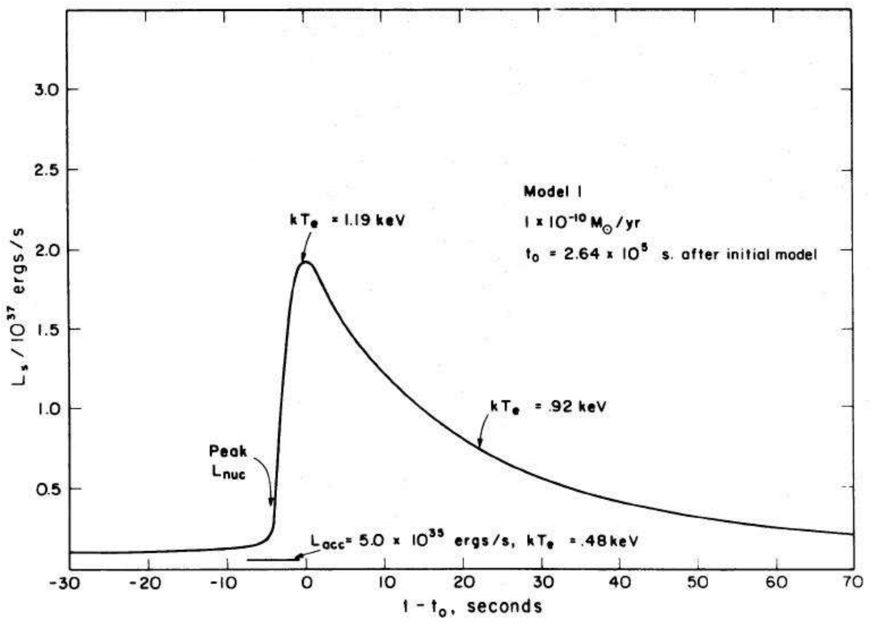

(Taam & Picklum, 1979, Fig. 2)

Theoretical outburst profile

Burst Theory, IV

The **Energy released** during the burst is:

$$E_{\mathrm{burst}} = Q\frac{4\pi R^2 H\rho}{m_{\mathrm{H}}} \sim 2 - 8 \times 10^{39}\,\mathrm{erg} \tag{6.7}$$

where typical parameters are $R = 10\,\mathrm{km}$, $H \sim 10^2\,\mathrm{cm}$, $\rho = 10^6\,\mathrm{g\,cm^{-3}}$, and

- H-burning: $Q = 7\,\mathrm{MeV\,nucleon^{-1}}$
- He-burning: $Q = 1.5\,\mathrm{MeV\,nucleon^{-1}}$

If the whole accreted matter $M_{\mathrm{acc}} = 4\pi R^2 H\rho$ is used, then the **time averaged burst luminosity** is

$$L_{\mathrm{burst}} = \frac{E_{\mathrm{burst}}}{\Delta t} = Q\frac{\dot{M}}{m_{\mathrm{H}}} \tag{6.8}$$

Since the **accretion luminosity** is

$$L_{\mathrm{acc}} = \frac{GM\dot{M}}{R} \tag{6.9}$$

the ratio between persistent and burst emission is

$$\alpha = 30 - 120 \left(\frac{M}{M_\odot}\right)\left(\frac{R}{10\,\mathrm{km}}\right)^{-1} \tag{6.10}$$

similar to what is observed.

$\alpha = 40$ for solar composition, $\alpha \gtrsim 100$ for pure He

Burst Theory, VI

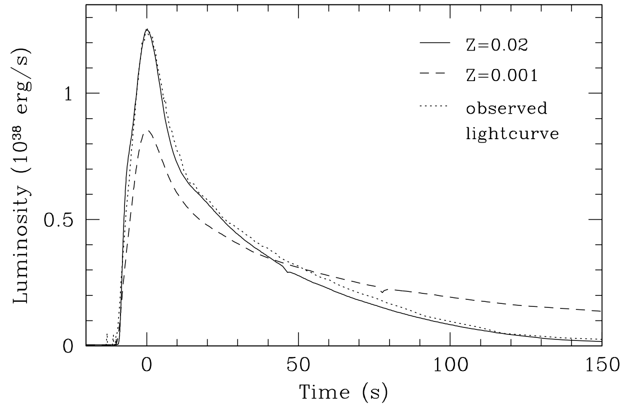

(Cumming, 2004, Fig. 3; calculation for average burst profile of GS 1826−24, the "clocked burster" with 4 h burst recurrence timescale)

Theory and observations of type I bursts agree well

Burst Theory, VII

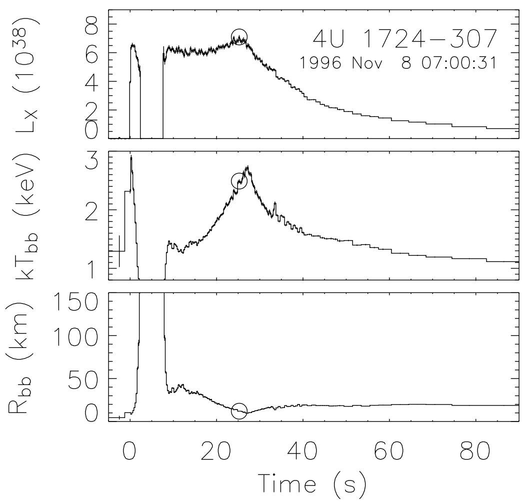

For most luminous bursts (large He fraction):

$L \gtrsim L_{\text{Edd}}$

$\Longrightarrow$ atmosphere "ejected"

$\Longrightarrow$ radius expansion bursts.

Note that outside of bursts $R_{\text{BB}} \sim R_{\text{neutron star}}$!

(Galloway et al., 2006, Fig. 10)

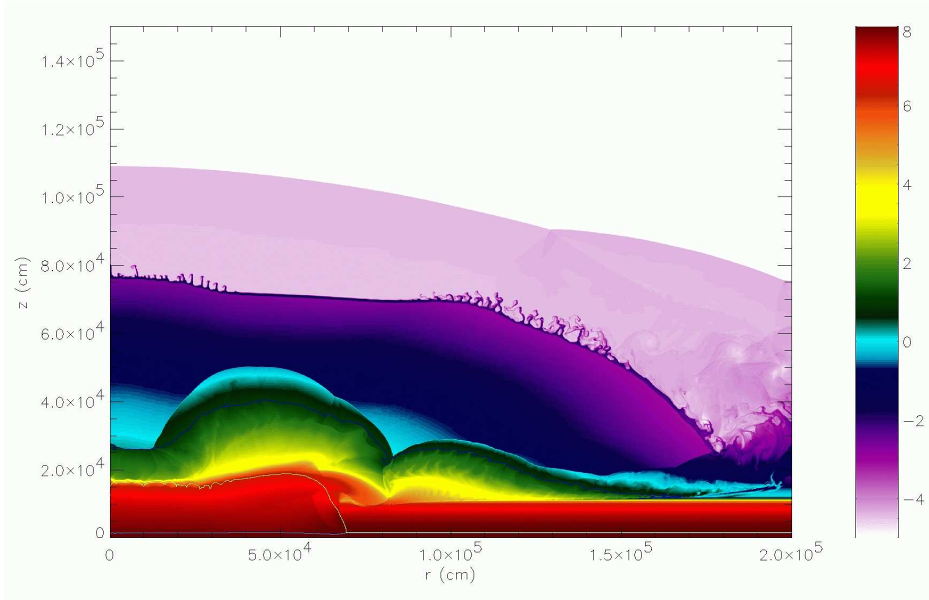

$t = 60\,\mu$s

Zingale et al. (2001): 2D hydrodynamical calculations of He detonation spreading over neutron star

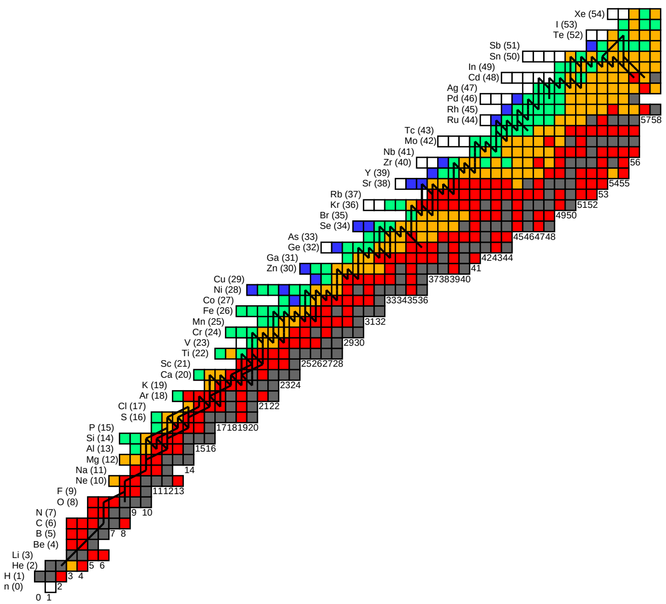

(Schatz & Rehm, 2006, Fig. 1)

For $T \gtrsim 10^9$ K, fusion of higher Z elements is possible during X-ray burst (rp-process)

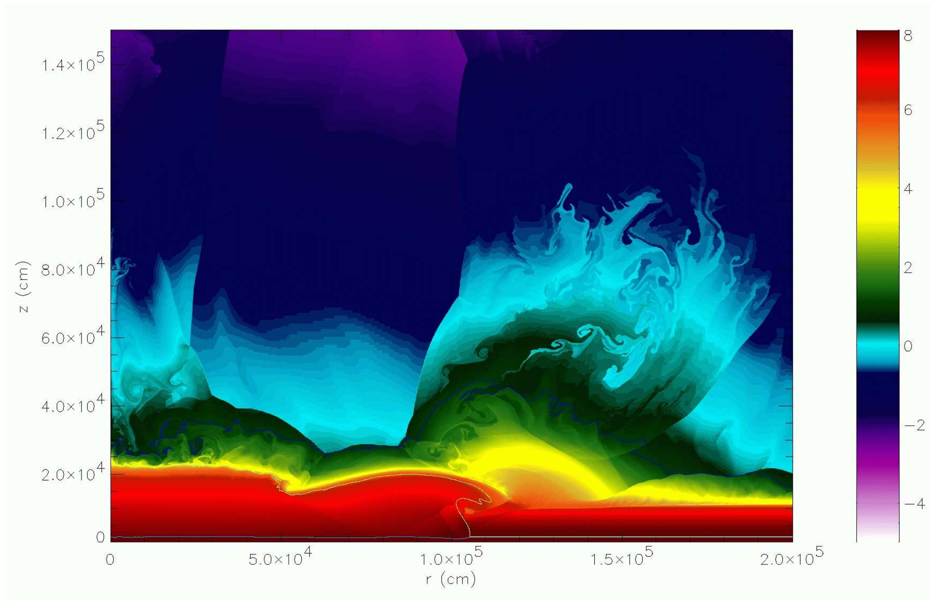

$t = 90\,\mu$s

Zingale et al. (2001): 2D hydrodynamical calculations of He detonation spreading over neutron star

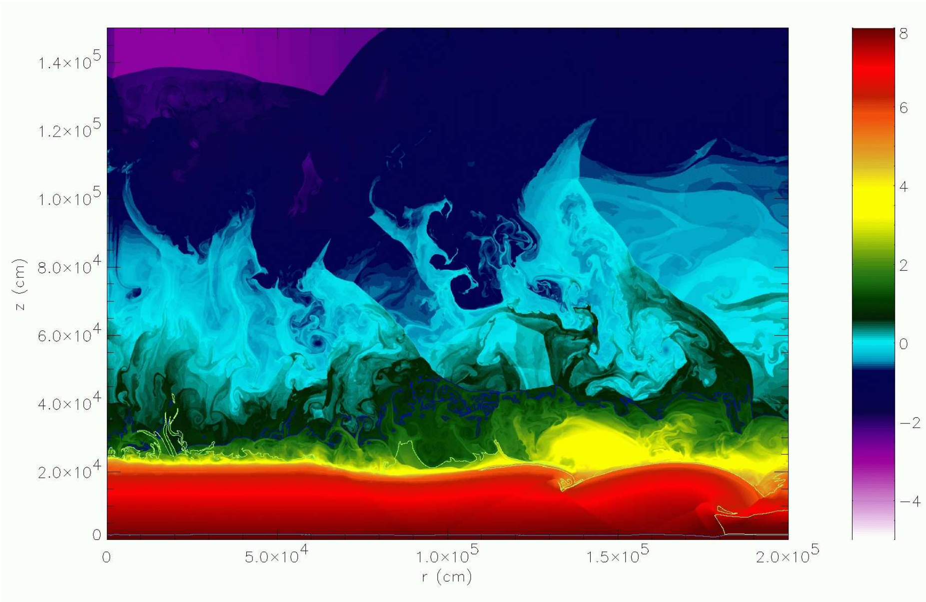

$t = 150\,\mu$s

Zingale et al. (2001): 2D hydrodynamical calculations of He detonation spreading over neutron star

Superbursts, I

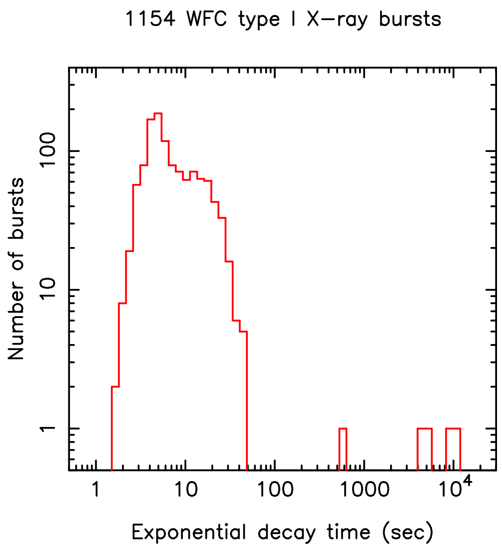

Some bursts have very long duration

(Kuulkers, 2004, Fig. 1)

Superbursts, II

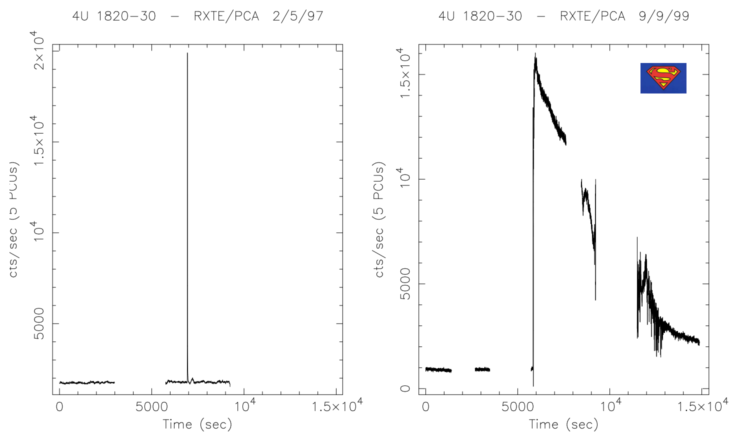

(Kuulkers, 2004, Fig. 3)

Some bursts have very long duration: Superbursts

Seen in 6 sources so far.

Superbursts, III

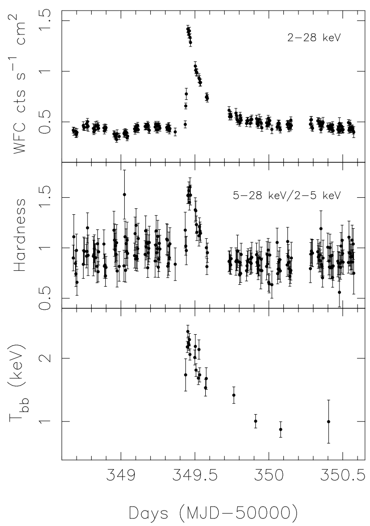

Temperature evolution over the superburst, similar to normal bursts, but the burst takes much longer $\Longrightarrow$ explosive C burning?

But: Early theory: pure ^{12}C layer is very stable, so would expect long recurrence time (100 s of years; Taam & Picklum 1979)

Cumming & Bildsten (2001): better theory: C burning is possible if there is a small ^{12}C fraction ($Z(^{12}\mathrm{C}) \sim 0.1$), so superbursts are probably signs of explosive carbon burning.

(Kuulkers, 2004, Fig. 2)